

Critical heat capacity near the nematic–smectic-*A* transition in octyloxycyanobiphenyl in the range 1–2000 bar

G. B. Kasting, K. J. Lushington, and C. W. Garland

*Department of Chemistry, Massachusetts Institute of Technology,
Cambridge, Massachusetts 02139*

(Received 26 December 1979)

An ac calorimetric technique has been used to study the nematic–smectic-*A* (*N*-*SmA*) and nematic-isotropic (*N*-*I*) transitions in octyloxycyanobiphenyl (8OCB) along a series of isobars between 1 atm and 2 kbar. The excess heat capacity $\Delta C_p(NA)$ associated with the essentially second-order *N*-*SmA* transition is found to diminish rapidly with pressure and is not observed for $p > 1.5$ kbar. The variation in $\Delta C_p(NA)$ with reduced temperature is not consistent with a logarithmic singularity but can be characterized by a critical exponent $\alpha = \alpha' = 0.25 \pm 0.05$ for all the pressures studied. The excess heat capacity at the *N*-*I* transition is almost independent of pressure; these data suggest but do not clearly establish quasitricritical behavior. Details of the experimental method and the fitting procedures are given.

I. INTRODUCTION

Liquid crystals are large, highly anisotropic organic molecules which melt in stages. Two of the more common intermediate phases between the solid and the isotropic (*I*) liquid are the orientationally ordered nematic (*N*) phase and the layered smectic-*A* (*SmA*) phase. The *N*-*SmA* phase transition has attracted considerable attention since the prediction by McMillan¹ that it could be second order in some cases. McMillan's result was obtained with the mean-field approximation; a more detailed treatment by de Gennes² placed the *N*-*SmA* transition in the $d=3$, $n=2$ universality class. (The complex order parameter ψ for the *SmA* phase involves the amplitude and the phase of a density wave; hence $n=2$ or *XY* model.) The short range of the intermolecular forces in liquid crystals leads to the prediction that the *N*-*SmA* transition should resemble the λ transition in ⁴He more closely than the normal-superconducting transition in metals. However, coupling between director fluctuations $\delta\bar{n}$ and the smectic order parameter ψ are predicted to make the transition always weakly first order.³ Recent analysis by Lubensky and Chen⁴ has shown that the behavior may be more complicated than that of a simple *XY* model with a first-order instability. They showed that a large splay elastic constant K_1 could lead to anisotropic quasitricritical behavior. On the basis of a postulated anisotropic scaling form for the correlation functions, they have developed a set of renormalization-group recursion relations for a generalized de Gennes model having an order parameter with $\frac{1}{2}n$ complex components. For small values of n (< 238.17) two fixed points exist—a trivial Gaussian fixed point, in which the order parameter ψ is completely decoupled from

$\delta\bar{n}$, and an n -component Heisenberg fixed point. For larger values of n , two more fixed points come into play. An isotropic superconducting fixed point corresponding to $K_1=0$ and leading to *XY* behavior is stable for $n > 365.9$. Another fixed point corresponding to $K_1=\infty$ exists for all $n > 238.17$ and leads to extremely anisotropic critical behavior. Furthermore, the transition at large n may be second-order. Hence, crossover behavior from mean-field to anisotropic-critical to isotropic-critical to a first-order transition, or some subsequence of the above, is possible. For $n=2$ it is suggested that quasitricritical behavior with the same types of crossover as for the large n case may occur until the inevitable first-order transition finally intervenes. Hence the observed or "effective" critical exponents may be nonuniversal and, in particular, there may be a physically accessible range dominated by quasitricritical anisotropic behavior that is not the same as the *XY* behavior of helium near its λ point.

Despite theoretical predictions of an intrinsically first-order transition, there are several experimental cases in which the *N*-*SmA* transition must be very close to second order. Much early work was done on *p*-cyanobenzilideneoctyloxylaniline (CBOOA), a bilayer smectic with a low *N*-*SmA* transition enthalpy (< 50 J mol⁻¹).^{5,6} Careful examination of this transition by dilatometry⁷ and by a variety of scattering techniques^{8,9} showed no detectable first-order discontinuities, despite a few earlier reports to the contrary.^{6,10} The scattering results were about evenly divided between mean-field critical correlation exponents ($\nu=0.50$) and heliumlike exponents ($\nu=0.67$), with some evidence for anisotropic behavior with $\nu_{\parallel} > \nu_{\perp}$.⁹ A temperature-pulse calorimetric technique⁵ yielded $\alpha \approx \alpha' \approx 0.15$ for the

specific-heat critical exponent, a result incompatible with both the mean-field and the XY ($\alpha = \alpha' \simeq -0.026$; almost logarithmic) model.

CBOOA is not an ideal material to study due to chemical instability of the Schiff's base linkage. Octyloxycyanobiphenyl (8OCB), the biphenyl analog of CBOOA, is a much more suitable material since it has excellent stability and is available in high purity from British Drug Houses Chemicals, Ltd. Detailed experiments have also shown the N -SmA transition in 8OCB to be second-order to within experimental accuracy.^{9,11} 8OCB is a bilayer smectic¹² showing reentrant nematic behavior at high pressures.¹³

We have carried out an ac calorimetric study of the N -SmA transition in 8OCB along a series of isobars between 1 and 2000 bar (see Fig. 1). A summary of these results has appeared elsewhere,¹⁴ but the experimental method and detailed fitting procedures have not been discussed previously. An earlier calorimetric study of this material at 1 atm by Johnson and co-workers¹⁵ yielded results that were interpreted as being consistent with a logarithmic singularity in C_p at the N -SmA transition. However, their sample had a 40-mK-wide two-phase coexistence region, and the resulting uncertainty in the location of T_{NA} lent an undesirable amount of freedom to the fits. Our data at 1 atm, while consistent with Johnson's outside of

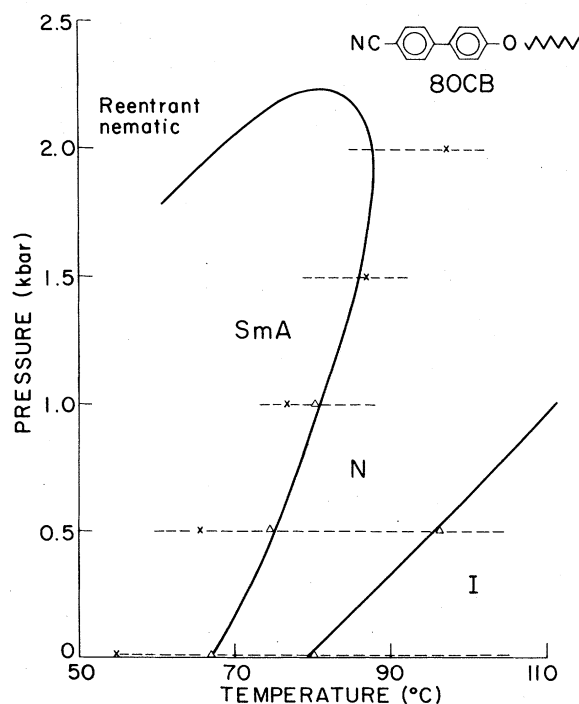


FIG. 1. Phase diagram of 8OCB. The dashed lines indicate the ranges over which C_p data were obtained, and the triangles indicate the transition temperatures obtained in this work. The solid phase lines are taken from Ref. 13. The x 's indicate the equilibrium melting point of the solid phase.

the two-phase region, have a considerably sharper C_p peak and clearly require a positive exponent α in the range 0.2–0.3. At higher pressures the C_p peak is markedly diminished in magnitude but retains basically the same shape.

This paper is organized as follows: The theory of the ac calorimetric method at atmospheric and high pressures is reviewed in Sec. II, the experimental details and data-reduction procedures are described in Sec. III, and the experimental results are presented in Sec. IV. The least-squares fitting procedures and the resulting critical exponents at the N -SmA transition are discussed in Sec. V; a brief analysis of the N -I transition appears in Sec. VI.

II. THEORY OF THE METHOD

The ac calorimetric technique has proven to be a useful method for studying second-order phase transitions¹⁶ and to be particularly well suited to high-pressure studies.^{17,18} In this section we review the basic principles of the method as applied at atmospheric and higher pressures and summarize its strengths and weaknesses. The development is closely related to that of Ref. 17, with substantial changes in notation to improve clarity.

The simplest model for an ac calorimeter is one in which a sample of heat capacity C_p is connected to a bath at reference temperature T_0 by a massless link with thermal conductance Λ

$$\Delta T_{dc} = \langle Q(t) \rangle / \Lambda \quad (1)$$

and an ac temperature oscillation $T(t)$. If the oscillatory part of the heat input has the simple form $Q_0 e^{i\omega t}$ and the period $2\pi/\omega$ is long compared with the time scale for heat flow in the sample, then $T(t)$ is given by

$$T(t) = \Delta T_{ac} e^{i(\omega t + \phi)}, \quad (2)$$

where

$$(Q_0 / \Delta T_{ac})^2 = (\omega C_p)^2 + \Lambda^2, \quad (3a)$$

$$\tan \phi = -\omega C_p / \Lambda. \quad (3b)$$

It is experimentally convenient to define a quantity C^* by

$$C^* \equiv Q_0 / \omega \Delta T_{ac}. \quad (4)$$

Then Eq. (3a) can be rewritten in the form

$$(C^* / C_p)^2 = 1 + (\Lambda / \omega C_p)^2. \quad (5)$$

At atmospheric pressure most experiments are operated in a frequency regime such that $\Lambda / \omega C_p \ll 1$, so that $C^* \simeq C_p$ is an excellent approximation.

In high-pressure ac calorimetry the sample is immersed in a necessarily dense pressure-transmitting

fluid which serves as the major source of heat loss. In this case the assumption that the thermal link Λ has negligible heat capacity is no longer valid, and one must take this fact into account. Finite thermal conductivity (or diffusivity) effects in the sample also become more important, due to the smaller thermal impedance mismatch with the surroundings. A simple model in which both these effects are taken into account is the following: A uniform slab of material of thickness l_2 , density ρ_2 , specific heat c_2 , and thermal-conductivity λ_2 is immersed in an infinite sea of material with thermal parameters ρ_1 , c_1 , and λ_1 . A heat flux density $\tilde{Q}_0 e^{i\omega t}$ is applied to one face of the sample ($x=0$) and the temperature is measured on the opposite face ($x=l_2$). If the lateral dimensions of the sample are large compared to its thickness, edge effects may be ignored and the problem may be treated as a one-dimensional heat conduction problem. In this case the temperature at the detector is given by¹⁹

$$T(l_2, t) = (\tilde{Q}_0 / \alpha_2 \lambda_2) [(1 + F^2) \sinh \alpha_2 l_2 + 2F \cosh \alpha_2 l_2]^{-1} e^{i\omega t}, \quad (6)$$

where

$$\alpha_j \equiv (i\omega \rho_j c_j / \lambda_j)^{1/2} \quad (7)$$

and

$$F \equiv \alpha_1 \lambda_1 / \alpha_2 \lambda_2 = (\rho_1 c_1 \lambda_1 / \rho_2 c_2 \lambda_2)^{1/2}. \quad (8)$$

This result can be recast into a form similar to Eq. (5) by defining C^* as before and introducing a complex quantity $Z = Z_{\text{Re}} + iZ_{\text{Im}}$ defined by

$$Z = [(1 + F^2) \sinh \alpha_2 l_2 + 2F \cosh \alpha_2 l_2] / \alpha_2 l_2. \quad (9)$$

Using these quantities and including a term Λ_l to take into account any additional heat loss through paths such as electrical leads, one finds for a slab of finite area that Eq. (6) can be rewritten as

$$(C^*/C_p)^2 = Z_{\text{Re}}^2 + [(\Lambda_l / \omega C_p) - Z_{\text{Im}}]^2. \quad (10)$$

The high-pressure analog of Eq. (3b) is found to be

$$\tan \phi = Z_{\text{Re}} / [Z_{\text{Im}} - (\Lambda_l / \omega C_p)]. \quad (11)$$

The quantity C_p is the total heat capacity of the slab, the quantity Q_0 appearing in the Eq. (4) definition of C^* is the total heat flux, and the parameters Z_{Re} and Z_{Im} represent contributions to C^* due to the pressure medium (gas) surrounding the cell. Note that in the limit of low gas density ($F \rightarrow 0$) and thin samples ($|\alpha_2 l_2| \ll 1$), we have $Z_{\text{Re}} \rightarrow 1$, $Z_{\text{Im}} \rightarrow 0$ and the one-atmosphere results are recovered.

The ac technique has several advantages for studying second-order or nearly second-order phase transitions: (i) The steady-state nature of the measurement permits one to remain at a given temperature indefinitely so that attainment of thermodynamic

equilibrium may be ensured even when relaxation times become very long; (ii) since data may be taken either on warming or cooling, hysteresis effects may be examined; (iii) the periodic nature of the signal permits the employment of sophisticated analog or digital signal averaging techniques for noise rejection; (iv) relatively small samples (1–100 mg) are required so that expensive or hard-to-prepare materials can be conveniently studied; and, finally, (v) the method may be used in the kilobar range with only modest corrections (30–50%) that are not sensitive functions of the temperature.

The ac technique does have some limitations. Though precision may be high, absolute accuracy is usually no better than 5% and is often worse. The method is time consuming, making it unattractive for exploratory work. The most serious drawback is that there is no reliable means of measuring latent heats or even detecting them with certainty. We have, however, found a close correlation between anomalous phase shifts in the T_{ac} signal and suspected two-phase regions at known first-order transitions in 8OCB and in other compounds.²⁰ The phase shift is always in a direction which corresponds to unusually rapid heat transfer within the sample. Such effects have been observed repeatedly in 8OCB at the solid-SmA and N - I transitions, but have never been seen at the N -SmA transition.

III. EXPERIMENTAL PROCEDURES

The ac calorimeters used in this work were similar to the one described in Ref. 17, with the addition of a sample cell designed for liquids, a computerized data-acquisition system, and a few smaller changes. In terms of precision and ease of operation, the new calorimeters were substantially better than the earlier version. This section describes our calorimeters and our method of collecting data.²¹

The sample cell was a specially constructed silver cell designed to meet the requirements of chemical inertness, low heat capacity, high thermal conductivity, and compatibility with high-pressure use. The body of the cell was a cup 1 cm i.d. \times 0.12 cm deep pressed from 0.010-in. silver sheet. A lid of 0.001-in. silver foil, soldered across the top of the cell, isolated the sample from the surrounding pressure medium but freely transmitted hydrostatic pressure. The ac heat input was supplied by a 30- Ω Chromel wire resistance heater epoxied to the base of the cup, and the temperature oscillations were detected by a small bead thermistor (Fenwal No. GB 43L1) cemented to the center of the lid. A carefully wound coil of fine gold wire placed in the cup along with the sample greatly increased the effective thermal conductivity of the package.

The empty cell weighed ~ 0.5 g and had a heat

capacity which was a smooth function of temperature over the range of the experiment (0–110 °C). The cell was filled under a dry nitrogen atmosphere by injecting with a glass syringe 70–100 mg of liquid crystal through a special filling port. This port was then sealed with a low-melting (117 °C) In-Sn-Pb solder in a manner such that the sample was kept cool (<80 °C) and isolated from the solder. The cell was then suspended by two AWG No. 28 copper leads in an outer sample holder which was mounted in one of the constant-temperature baths. The loaded cell had a heat capacity of 0.30–0.35 J K⁻¹, 50 to 60% of which was due to the liquid crystal. The 8OCB was used as received from BDH Chemicals since the manufacturer's stated purity was 99.5% minimum.

Two different regulated temperature baths were used in these experiments. The one-atmosphere runs were carried out in a Luda NBS circulating bath regulated by a Tronac Model 40 temperature controller. Short-term temperature stability was estimated to be ±3 mK in the bath but was considerably better (±1 mK over the duration of a 20 minute data point) at the location of the sample cell due to an appropriate amount of thermal isolation of the cell from the bath. Temperature gradients across the cell due to the dc component of the heat input have been estimated to be <0.2 mK at 1 atm and <1 mK at 3 kbar. Absolute temperatures were provided by a Leeds and Northrup 8164-B platinum resistance thermometer mounted in an aluminum block attached to the sample holder and were accurate to within ±20 mK.

The high-pressure runs were carried out in a separate calorimeter. In this case the sample cell was mounted on a copper strut which was suspended in a massive (23 kg) steel pressure vessel. The pressure "bomb" was immersed in a large circulating oil bath regulated by another Tronac controller. Temperature stability was virtually identical with that of the one-atmosphere calorimeter, both in the bath and at the sample. Absolute temperatures were again provided by an L and N 8164-B thermometer, which in this case was mounted in the oil bath outside the pressure bomb. Due to possible temperature gradients between the inside and outside of the bomb, absolute accuracy is estimated to be only ±50 mK.

The pressure medium was Airco welding-grade argon, pumped to a maximum pressure of 3 kbar by a two-stage Harwood gas compressor. Pressure was measured with a calibrated manganin coil and could be maintained constant to better than 5 bar over the duration of a four-week long high-pressure run. The readability and short-term stability were considerably better, so that pressure stability during a one-day scan through a phase transition was estimated to be ±0.3 bar. Absolute accuracy in the pressure values was ±30 bar.

Data collection was handled in the following manner. A very stable low-frequency oscillator pro-

vided a sinusoidal heat input to the sample. The resulting temperature oscillations, having a frequency of 0.033 Hz ($\omega = 0.207$) and peak-to-peak amplitude of 8–10 mK, were detected by the thermistor, which comprised one arm of a sensitive ac resistance bridge. This bridge was driven at ~1050 Hz, and the temperature oscillations in the sample created an imbalance signal in the bridge, which was converted to a slow sinusoidal variation in the output of the lock-in amplifier that served as the null detector. This signal was digitized and stored in the memory of an IMSAI 8080 microcomputer. Successive periods were overlaid in memory until 40 periods (20 min) of data had been collected. The amplitude and phase of the averaged signal were then determined by performing Fourier sine and cosine sums over the stored data. Finally the average temperature and the effective heat capacity C^* were computed and these results stored on a flexible disk for further analysis.

One additional step in the data-acquisition process is worth noting. When the ac temperature signal was analyzed as described above, the largest source of scatter in the data was slow drifts in the bath temperature associated with imperfect temperature control. These random drifts, while small (<1 mK), still correspond to a variation that was ~10% of the ac amplitude. Their effect could be practically eliminated, however, by computing the average temperature during each period of the ac oscillation, reconstructing the bath temperature drift from these averages and correcting the Fourier amplitude for the drift. When analyzed in this manner, the scatter in our C^* values was ~0.06%. The one-atmosphere data are easily converted to C_p values using Eq. (5). We tested the validity of this equation for our system by measuring the frequency dependence of ΔT_{ac} . A plot of $(Q_0/\Delta T_{ac})^2$ vs ω^2 was linear for $0.06 < \omega < 0.3$, which implies that the data are well described by Eqs. (3a) or (5) over this range. The parameter Λ can be determined from the $\omega = 0$ intercept of the above plot or calculated directly from the length and cross section of the heater leads. The same result, $\Lambda = 0.008 \pm 0.001$ watt K⁻¹, was obtained using both methods. Thus $\Lambda/\omega C_p < 0.13$ at $\omega = 0.207$ (our standard operating frequency) and C_p differs from C^* by less than 0.8%.

Reduction of the high-pressure data is not quite as straightforward. Clearly the actual geometry of the sample cell and its surroundings are more complex than that of the model presented in Sec. II. The sample is not a uniform slab of a single material and is too thick for the one-dimensional heat-flow model to be strictly applicable. Rather than developing a complex model (which might involve more parameters than could be uniquely determined), we have used the model represented by Eqs. (6)–(11) with the simplifying assumption that the noncritical (background) heat capacity of the sample plus the con-

tainer is independent of pressure. Λ_1 and the sample thickness l_2 can be measured directly, and the high-pressure thermal properties of argon (ρ_1, c_1, λ_1) are well known.²² We find, away from the vicinity of transition points, that the observed values of C^* over wide ranges in pressure and frequency can be well represented by using an effective cell thermal conductivity λ_2 and an effective cell density ρ_2 that are independent of pressure and temperature. For the range $0 < p < 2$ kbar, $55 < T < 105$ °C, and $0.1 < \omega < 0.9$, we used $\lambda_2 = 0.0113$ W cm⁻¹ K⁻¹ and $\rho_2 = 2.28$ g cm⁻³. These values are quite consistent with the high-frequency rolloff of the $(Q_0/\Delta T_{ac})^2$ -vs- ω^2 plot at 1 atm and yield high-pressure C_p values that are independent of pressure (within $\pm 5\%$) when the sample is not close to any phase transition. The above values of λ_2 and ρ_2 were then used in conjunction with Eqs. (9) and (10) to reduce high-pressure C^* values to C_p values [$C_p = m_2 c_2(T)$, where m_2 is the mass of the loaded cell and $c_2(T)$ is its average specific heat at temperature T].

One troublesome feature of the data should be pointed out. Several of the runs contained one or two abrupt systematic changes of 0.3–0.8% in the C^* values, well above the normal scatter of 0.06%. In each case the C^* values at temperatures above and below the break followed parallel curves which could be superimposed by making a small additive correction. We believe these breaks were caused by either a change in the domain pattern (and hence, the effective thermal conductivity) of the sample or a mechanical instability in the thin foil lid to which the thermistor was attached. The data shown below have been corrected for such effects.

IV. RESULTS

We have measured the heat capacity of 80CB along five isobars over the temperature ranges shown in Fig. 1. These measurements were carried out in order of ascending pressure, with a second 1-atm run being made after the high-pressure runs. Data were taken on warming and on cooling, with no discernible difference between the two sets. The N - SmA transition temperature did not change between the initial and final 1-atm runs (a period of more than 4 months); however, a small shift of ~ 20 mK was observed over a two-week period during the final run. Since data very near the transition were always taken during a 1–2 day period, this drift had a negligible effect on the results. At 500 and 1000 bar the N - SmA transition temperature obtained from several runs at each pressure was reproducible to better than 20 mK (corresponding to a pressure stability of ~ 2 bar). This stability in the transition temperature plus the fact that the cell was depressurized from 2 kbar without damage provide convincing evidence that the

sample remained isolated from the argon pressure medium throughout the experiment.²³

The location of the phase boundary between the smectic- A and nematic phases at high pressures has been found to be sample dependent.¹³ The curve shown in Fig. 1 corresponds to the sample in Ref. 13 with the largest region of smectic stability, which was believed to be the purest of those studied. Our sample gave transition temperatures for $p \leq 1000$ bar that were very close to this curve, suggesting that the transition temperatures should be similar at higher pressures as well. However, as shown below, no thermal anomaly associated with the N - SmA transition could be detected at 1500 or 2000 bar. It was also not possible to study the re-entrant nematic portion of the phase diagram due to spontaneous crystallization of the supercooled smectic- A phase over the long time scale of our measurements.

In terms of integrated enthalpy, the N - I transition is much larger than the N - SmA transition. Figure 2 shows the variation in C_p associated with the N - I transition at 1 atm and at 500 bar. The shape and magnitude of this peak are insensitive to small amounts of impurity (data are shown at 1 atm for both the investigated sample and a less pure sample with a lower T_{NI} value) and are almost independent of pressure. The small differences observed when $T - T_{NI} < -10$ K may be due to the increase in the nematic order parameter S (and a corresponding decrease in its fluctuations) upon cooling through the N - SmA transition at 1 atm. The heat capacity in the vicinity of the N - SmA transition is shown in Fig. 3. This C_p peak diminishes rapidly with increasing pressure and is not detectable at 1.5 kbar and above. The

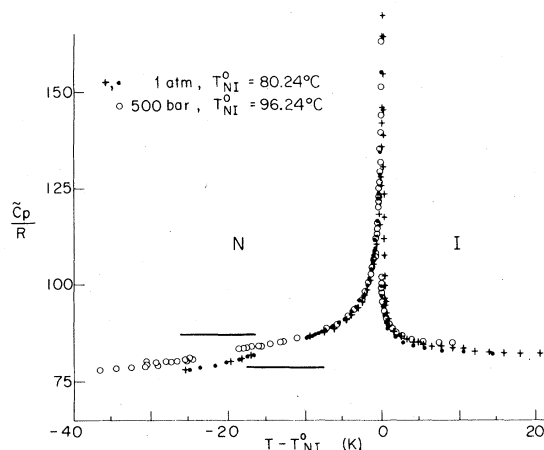


FIG. 2. Heat capacity of 80CB (MW = 307.44) in the vicinity of the N - I transition at 1 atm and 500 bar. A detailed view of C_p over the ranges indicated by the horizontal lines is shown in Fig. 3. T_{NI}^0 denotes the observed temperature of the weakly first-order transition. Data points close to the N - SmA transitions have been omitted for clarity.

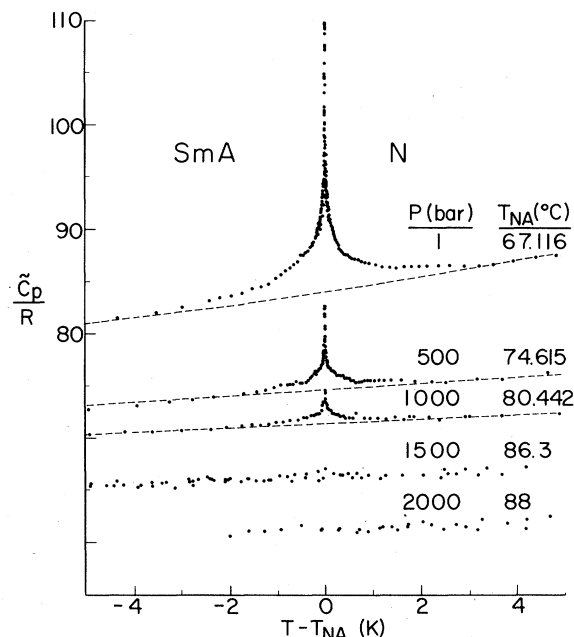


FIG. 3. Heat capacity of 8OCB in the vicinity of the N - SmA transition for the five isobars shown in Fig. 1. The data at 500, 1000, 1500, and 2000 bar are shifted down by 5, 10, 15, and 20 units, respectively. The background C_p curves used in the power-law fits are indicated by dashed lines.

same behavior has been observed in several other samples of 8OCB and in the related material octylcyanobiphenyl (8CB),²⁴ a bilayer smectic which does not exhibit re-entrant behavior. The trend in the excess entropy δS_{NA} for 8OCB¹⁴ is qualitatively similar to the decrease in transition entropy with decreasing T_{NA}/T_{NI} predicted by mean-field theory,¹ particularly in the version of Lee *et al.*²⁵ However, it should be stressed that our results do *not* correspond to a decrease in the latent heat but rather to a decrease in the *pretransitional* entropy associated with the N - SmA transition. A possible explanation of this effect of pressure would be that the excess N - SmA entropy is mainly due to nematic order parameter fluctuations, which are expected to decrease with increasing $T_{NI} - T_{NA}$.²⁶ A similar argument has been presented by Brisbin *et al.*²⁷ to explain the size of the C_p peaks at the N - SmA transition in the homologous series $\bar{n}S.5$.

The dashed curves shown in Fig. 3 are smooth interpolations of the N - I heat-capacity peak through the region of the N - SmA transition. The critical heat capacity $\Delta C_p(NA)$ associated with the N - SmA transition is the difference between the observed data and the noncritical background curve. This choice of background is both physically plausible and consistent with a power-law variation for ΔC_p .

Before discussing the details of the fitting procedure, we present in Fig. 4 a comparison of the 1-

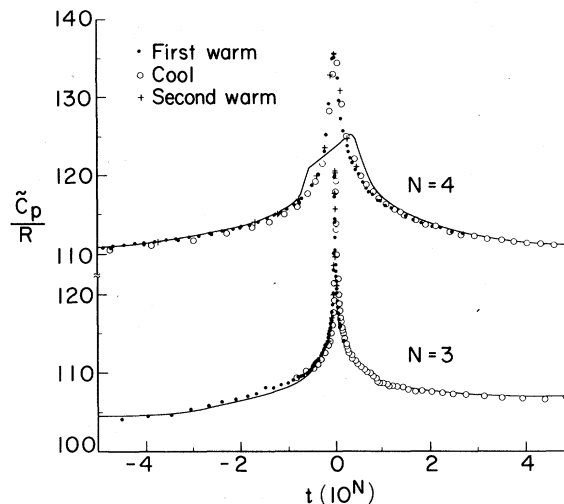


FIG. 4. Heat capacity of 8OCB near the N - SmA transition at 1 atm. The present data have been normalized to agree with Ref. 15 by multiplying by the factor 1.236. The temperatures of the data represented by \circ and $+$ have been shifted 23 mK to compensate for a change in T_{NA} between the first warming run and the cooling run. The solid curve accurately describes the data presented in Ref. 15.

atm data near T_{NA} with the earlier results of Johnson *et al.*¹⁵ Aside from the existence of a 40-mK-wide coexistence region in Johnson's data and a fairly substantial (24%) difference in absolute values, the variations in C_p are very similar. A recent reinvestigation by Johnson of a high-purity 8OCB sample confirms the rapid variation in C_p near T_{NA} reported here.²⁸

Another comparison of interest is to the results of differential scanning calorimetry (DSC), which yields values of 25–60 J mol⁻¹ for the heat of the N - SmA transition in 8OCB.²⁹ It is common practice to quote such DSC enthalpies as latent heats although the DSC method cannot distinguish truly discontinuous changes in enthalpy H from rapid but continuous variations. The DSC method is also subject to difficulties associated with equilibrium near a transition (typical scanning rates are 2.5–5 K/min) and choice of base line.²⁹ As a result, DSC heats are mainly of qualitative value. The ac method yields good equilibrium values of the excess heat capacity ΔC_p but cannot measure latent heats. However, anomalous shifts in the phase ϕ of the T_{ac} signal can provide an indication of the coexistence of two phases.²⁰ We see such two-phase behavior close to the weakly first-order N - I transition, but there are no indications of phase coexistence at the N - SmA transition. The excess enthalpy $\delta H \equiv \int \Delta C_p dT$ due to pretransitional (critical) contributions is 100 J mol⁻¹ at 1 atm. If there is any very weak first-order character at the N - SmA transition, we anticipate that the latent heat will

be less than 5 J mol^{-1} (thus $\Delta S < 0.0018R$ for the corresponding discontinuous entropy change).

V. DISCUSSION

A. Fitting procedure

The Marquardt algorithm³⁰ has been used to fit the data to functions of the form

$$\Delta \bar{C}_p/R = \begin{cases} A|t|^{-\alpha} + B & \text{for } T > T_{NA} \text{ ,} & (12a) \\ A'|t|^{-\alpha'} + B' & \text{for } T < T'_{NA} \text{ ,} & (12b) \end{cases}$$

where $t = (T - T_{NA})/T_{NA}$. The quality of a fit is specified in terms of the reduced χ square

$$\chi_v^2 = \frac{1}{\nu} \sum_{i=1}^n \frac{1}{\sigma_i^2} [y_i(\text{obs}) - y_i(\text{calc})]^2 \text{ ,} \quad (13)$$

where y denotes $\Delta \bar{C}_p/R$ and $\nu = n - p$ is the number of degrees of freedom (n being the number of data points and p the number of adjustable parameters). Our data were found to be consistent with a constant standard deviation $\sigma_i = 0.12$ (equal weights) for $|t| > 3 \times 10^{-5}$,³¹ which is the smallest t value for which the data are only weakly affected by possible systematic errors due to the finite amplitude of the temperature oscillations.³²

Table I shows the results of fitting separately the data above and below T_{NA} to Eq. (12) over three different ranges of reduced temperature. Corrections-to-scaling terms have not been included in Eq. (12) since good fits may be obtained without them, but the effect of such terms will be discussed later. The error bounds for α given in Table I and subsequent tables are 95% confidence limits based on the F test. They were determined by fixing α at several values different from the optimum (α_0), minimizing χ_v^2 at the new α value (α_1), calculating the ratio $\chi_v^2(\alpha_1)/\chi_v^2$

TABLE I. Critical parameters obtained from separate fits with Eqs. (12a) and (12b) to the data above and below the N -SmA transition. The reduced temperature ranges are: (1) $1 \times 10^{-5} < |t| < 1 \times 10^{-2}$, (2) $3 \times 10^{-5} < |t| < 3 \times 10^{-3}$, (3) $3 \times 10^{-5} < |t| < 1 \times 10^{-3}$. A bracket indicates that the parameter was held fixed at the indicated value.

Data set	Temp range	ν	A (A')	α (α')	B (B')	T_{NA} (T'_{NA})	χ_v^2
1 atm							
$T > T_{NA}$	1	86	1.20	0.27 ± 0.03	-3.82	[67.116]	1.09
	2	68	1.17	0.27 ± 0.04	-3.72	[67.116]	1.15
	2	67	1.26	$0.26 \begin{smallmatrix} +0.13 \\ -0.11 \end{smallmatrix}$	-3.93	67.116	1.16
$T < T_{NA}$	3	55	1.11	0.27 ± 0.07	-3.48	[67.116]	1.25
	1	81	2.37	0.20 ± 0.06	-5.61	[67.116]	4.70
	2	66	3.14	0.18 ± 0.06	-6.64	[67.116]	1.60
	2	65	11.76	$0.09 \begin{smallmatrix} +0.17 \\ -0.06 \end{smallmatrix}$	-17.76	67.111	1.38
	3	57	1.82	0.22 ± 0.11	-3.96	[67.116]	1.42
	1	80	0.89	0.27	-1.57	[67.116]	3.09 ^a
2	65	0.97	0.26	-1.41	[67.116]	1.31 ^a	
500 bar							
$T > T_{NA}$	1	53	0.345	0.28 ± 0.07	-1.19	[74.615]	0.76
	2	40	0.290	0.29 ± 0.11	-1.03	[74.615]	0.58
	2	39	0.678	$0.22 \begin{smallmatrix} +0.32 \\ -0.20 \end{smallmatrix}$	-1.86	74.618	0.55
$T < T_{NA}$	3	27	0.118	0.37 ± 0.12	-0.23	[74.615]	0.31
	1	44	0.247	0.31 ± 0.09	-0.93	[74.615]	1.60
	2	35	0.267	0.30 ± 0.14	-0.88	[74.615]	0.99
	2	34	0.273	$0.29 \begin{smallmatrix} +0.70 \\ -0.28 \end{smallmatrix}$	-0.89	74.615	1.02
	3	25	0.245	0.30 ± 0.23	-0.75	[74.615]	0.76
1000 bar							
$T > T_{NA}$	2	15	1.06	0.14 ± 0.22	-2.26	[80.442]	0.38
$T < T_{NA}$	2	13	0.224	0.26 ± 0.58	-0.74	[80.442]	1.35

^aDifferent choice of background ($E' = 202$ for range 1, 360 for range 2); see text for details.

(α_0), and comparing this with the limiting value of $F(\nu, \nu)$. This procedure yields error bounds several times larger than the standard parameter errors obtained directly from the least-squares fitting routine. The rather large bounds at 1000 bar reflect the fact that this very small C_p peak was close to the limits of our experimental resolution.

For most of the fits in Table I, T_{NA} and T'_{NA} have been fixed at T_m , the temperature of the C_p maximum. These fits are stable to range shrinking and yield parameters that are roughly consistent with the scaling requirements $\alpha = \alpha'$ and $B = B'$. The largest discrepancy occurs at 1 atm, where α' is smaller than α and the fit over the full three decades in t (range 1) is very poor for the SmA phase. Deviation plots show substantial systematic deviations in the SmA phase at 1 atm when $|t| < 3 \times 10^{-5}$. It would be tempting to suggest that this may be a consequence of the finite T_{ac} amplitude³²; but such an effect is not seen in the N phase.

One variation of the fitting procedure is to allow T_{NA} and T'_{NA} to be adjustable parameters in the least-squares fit with Eq. (12). The resulting critical parameters are shown in Table I for 1 atm and 500 bar data. (Fits at 1000 bar are unstable when T_{NA} and T'_{NA} are free parameters.) The fit improves only for the SmA phase at 1 atm, where T'_{NA} assumes a value 4.5 mK below T_m . Although the SmA deviations are reduced at both ends of the $|t|$ range, we believe this fit is artificial since the resulting exponents clearly violate scaling and the low value $\alpha' = 0.09$ deviates from the values obtained at high pressures. The fact that the shifts in T_{NA} and T'_{NA} relative to T_m are very small and show no systematic pattern indicates that any two-phase region or first-order "gap" $T_{NA} - T_m$ must be insignificant (< 3 mK). For all the remaining fits, we will neglect the possibility of a very weak first-order character and will use $T_{NA} = T'_{NA}$.

A second variation of the fitting procedure is to consider a different choice for the background heat capacity. This can be accomplished in an equivalent

way by adding the terms Et to Eq. (12a) and $E't$ to Eq. (12b). In the nematic phase, the least-squares fit rejects the addition of such a term in Eq. (12a) at 1 atm and at 500 bar. Indeed, the nematic fits cannot be significantly improved by any change in the background. In the smectic phase, a change in background causes only an insignificant change in α' at 500 bar but a marked change at 1 atm. Significant improvements in the quality of the fits, and α' values in accord with scaling, can be achieved at 1 atm by using $E' \approx 300$ (see Table I). Although this procedure is rather *ad hoc*, it is consistent with the hypothesis that apparent deviations from scaling at 1 atm are due to complications in the SmA behavior when the N-I transition is close to the N-SmA transition. In this case, there are large variations of the nematic order parameter S in the SmA phase near T_{NA} that do not occur when $T_{NI} - T_{NA}$ is large and S is almost saturated prior to smectic ordering.^{1,26}

For a better test of the compatibility of our data with scaling, data above and below T_{NA} were fitted simultaneously using the constraints $\alpha = \alpha'$ and $B = B'$. The temperature range $3 \times 10^{-5} < |t| < 3 \times 10^{-3}$ was chosen as being least susceptible to systematic errors at either very large or very small $|t|$ yet still large enough to yield a meaningful result. In addition to the simple power-law form given by Eq. (12), we have also tested the form

$$\Delta \tilde{C}_p/R = \begin{cases} A|t|^{-\alpha}(1 + D|t|^{1/2}) + B & \text{for } T > T_{NA} , \\ A'|t|^{-\alpha}(1 + D'|t|^{1/2}) + B & \text{for } T < T_{NA} , \end{cases} \quad (14a)$$

$$(14b)$$

since the inclusion of corrections-to-scaling terms can have an effect on the α values. The results of these fits, where $T_{NA} = T'_{NA}$ is *not* constrained to equal T_m , are shown in Table II. It is obvious that the correction terms play an important role only at 1 atm, where the χ^2_v surface for fits with Eqs. (14) is very flat and α values ranging from 0.25 to 0.45 would be as good as the $\alpha = \alpha' = 0.3$ value shown. In addition

TABLE II. Critical parameters obtained on simultaneously fitting data above and below the N-SmA transition with the constraints $\alpha = \alpha'$ and $B = B'$. The range of the fits is $3 \times 10^{-5} < |t| < 3 \times 10^{-3}$.

P(bar)	A	A'/A	α	B	D/D'	T_{NA}	χ^2_v
1	2.446	1.016	0.20 ± 0.05	-6.04	...	67.119	2.09
	0.656	0.925	[0.30]	1.50	-17.43/-14.07	67.117	1.50
500	0.286	1.013	0.29 ± 0.10	-0.98	...	74.616	0.76
	0.277	0.975	0.30	-0.92	-0.83/0.45	74.615	0.77
1000	0.409	1.015	0.21 ± 0.27	-1.18	...	80.440	0.80
	0.862	0.969	0.17	-2.40	2.40/3.97	80.438	0.80

to the modest improvement in χ^2_ν , there are two other attractive aspects of using Eqs. (14) rather than Eqs. (12) at 1 atm: the least-squares value of T_{NA} is much closer to T_m , and the α value agrees better with the α values at high pressures. One should also note that the unconstrained values of D and D' come close to satisfying the universal ratio of unity expected for correction-to-scaling amplitudes.³³

As a final test of the data we wish to determine how well a single exponent α can describe the data at all three pressures. A simple power law, Eqs. (12), is used at high pressures and a form with corrections-to-scaling terms, Eqs. (14), is used for the 1-atm data. Table III gives the results of these fits. When all three data sets are considered, it is evident that the optimum α lies somewhere in the range 0.20–0.30. For comparative purposes we have included a fit with an Ising exponent and one for an exponent near the XY value. We conclude that the data at all three pressures are generally consistent with $\alpha = \alpha' = 0.25 \pm 0.05$ but are not consistent with the nearly logarithmic singularity associated with the XY model. Furthermore the data show no indication of crossover behavior in the 10^{-2} – 3×10^{-5} range except perhaps for the ordered phase at 1 atm where there are complications not yet understood.

B. Interpretation

One possible interpretation of the α values cited above is that the data are being influenced by a tri-

critical point somewhere along the N - SmA transition line (perhaps at a negative pressure for 8OCB). In this case an effective $\alpha \approx 0.25$ might represent crossover from tricritical behavior ($\alpha = 0.50$) to asymptotic XY behavior ($\alpha \approx -0.026$). Brisbin *et al.* proposed such an interpretation for the behavior of \tilde{C}_p in $\bar{9}S.5$.²⁷ However, we see no direct evidence for crossover behavior in 8OCB, either on range shrinking the data at a given pressure or on examining the trend in α with increasing pressure. It is, of course, conceivable that there is some complicated crossover sequence⁴ that eludes observation; but we will make a case below for considering $\alpha \approx 0.25$ as a single quasicritical exponent.

In the Lubensky-Chen model, crossover is predicted from quasicritical anisotropic to quasicritical isotropic to first order as $|t| \rightarrow 0$. However, numerical calculations⁴ suggest that an extensive range of quasicritical anisotropic behavior can exist, and our data suggest that any eventual crossover to isotropic XY behavior must occur extremely close to T_{NA} . Thus we will consider the behavior expected from the anisotropic fixed point. The modified version of hyper-scaling associated with this fixed point

$$2 - \alpha = \nu_{\parallel} + 2\nu_{\perp} \quad (15)$$

provides a link between the heat-capacity exponent and the critical exponents for the longitudinal and transverse correlation lengths. Thus a large value of α implies that the scattering data should also show

TABLE III. Result of fitting the data at the N - SmA transition at all three pressures with the same critical exponent α . The range of the data used in these fits is $3 \times 10^{-5} < |t| < 3 \times 10^{-3}$.

P (bar)	A	A'/A	α	B	D/D'	T_{NA}	χ^2_ν
1	0.656	0.925	[0.30]	1.50	-17.43/-14.07	67.117	1.51
500	0.258	1.013	[0.30]	-0.89	...	74.616	0.76
1000	0.145	1.023	[0.30]	-0.54	...	80.440	0.84
1	1.276	0.972	[0.25]	-2.11	-5.40/-3.20	67.118	1.57
500	0.471	1.010	[0.25]	-1.49	...	74.616	0.81
1000	0.262	1.018	[0.25]	-0.86	...	80.440	0.78
1	2.671	0.979	[0.20]	-6.92	0.30/1.93	67.118	1.63
500	0.890	1.007	[0.20]	-2.38	...	74.616	1.06
1000	0.487	1.021	[0.20]	-1.33	...	80.441	0.77
1	11.61	1.000	[0.11]	-22.78	2.21/2.59	67.119	1.95
500	3.34	1.008	[0.11]	-5.99	...	74.617	1.93
1000	1.81	1.014	[0.11]	-3.24	...	80.442	0.86
1	-220.16	0.989	[-0.02]	191.96	-0.574/-0.581	67.120	3.03
500	-51.52	0.998	[-0.02]	46.06	...	74.618	4.13
1000	-27.21	0.997	[-0.02]	24.33	...	80.444	1.23

TABLE IV. Results of separate fits above and below the N - I transition. T_{NI} and T'_{NI} are the "critical" temperatures determined from the power-law fits. The observed first-order transition temperatures T_{NI}^0 are 80.24 °C at 1 atm and 96.24 °C at 500 bar.

P (bar)	Temp range	$ t _{\min}$	$ t _{\max}$	A (A')	α (α')	B (B')	T_{NI} (°C) (T'_{NI})	χ^2_{ν}
1	$T > T_{NI}$	4.5×10^{-4}	3.1×10^{-2}	2.257	0.31 ± 0.09	-0.598	80.106	0.40
	$T < T_{NI}$	3.8×10^{-4}	2.9×10^{-2}	1.739	0.48 ± 0.13	-3.24	80.283	9.23
500	$T > T_{NI}$	5.4×10^{-4}	2.0×10^{-2}	0.986	$0.42^{+0.27}_{-0.18}$	-1.35	96.039	1.14
	$T < T_{NI}$	5.4×10^{-4}	5.3×10^{-2}	1.715	0.49 ± 0.04	-2.99	96.338	1.48

deviations from helium (XY) behavior. The general pattern of light scattering and x-ray scattering results in three bilayer smectics (8CB, 8OCB, and CBOOA) is $\nu_{\perp} < \nu_{\parallel} \approx \nu_{\text{He}}$.^{9,34} Unfortunately, the value of ν_{\parallel} is better determined experimentally, but we are more interested in ν_{\perp} . The best available values of ν_{\perp} are 0.58 ± 0.04 for 8OCB, 0.51 ± 0.04 for 8CB, and 0.62 ± 0.05 for CBOOA, all based on fits over the range $10^{-4} < |t| < 10^{-2}$.^{9,34} If we assume $\alpha = 0.25 \pm 0.05$ and use $\nu_{\parallel} = \nu_{\text{He}} = 0.675$, Eq. (15) would yield $\nu_{\perp} = 0.538 \pm 0.025$, which is reasonably close to the experimental values. Further progress will depend on a detailed development of the theory for parameters appropriate to the case of 8OCB.

As a final point, one can consider the implications of the dramatic pressure dependence of $\Delta C_p(NA)$ in terms of two-scale-factor universality.³⁵ By analogy with isotropic systems, one would expect the quantity $A \xi_{\parallel 0} \xi_{\perp 0}^2$ to have the same constant value at every pressure. Since the amplitude A of the critical heat capacity decreases markedly with pressure, coefficients of the correlation lengths should increase. It would be interesting to test the universality of $A \xi_{\parallel 0} \xi_{\perp 0}^2$ by carrying out scattering determinations of ξ at high pressures. This would be a valuable test in view of the apparent nonuniversality of $A \xi_0^3$ along the λ line in ^4He , where ξ_0 is independent of pressure but A decreases as the pressure increases.³⁶

VI. N - I TRANSITION

On the basis of the Landau model of de Gennes³⁷ the N - I transition is expected to be weakly first order, as observed experimentally. Keyes³⁸ has suggested, however, that effective tricritical exponents should be observed due to the presence of a nearby tricritical point under an applied field when the anisotropy in either the electric or magnetic susceptibility of the liquid crystal is negative.³⁹ A recent experimental study⁴⁰ of the gap exponent in p -methoxy

benzylidene p -butylaniline (MBBA) seems to support this conjecture.

The data shown in Fig. 2 show pronounced pre-transitional effects in the isotropic phase, which already demonstrates the inadequacy of a purely mean-field description of this transition. To test the compatibility of the data with quasitricritical behavior, we have separately fit the data above and below the N - I transition to Eq. (12). A linear background heat capacity $\tilde{C}_p(\text{bkgd})/R = a + 0.075T$, where $a = 75.48$ at 1 atm and 70.55 at 500 bar was subtracted from the data to obtain $\Delta \tilde{C}_p/R$. Since the transition is weakly first order, the constraints $B = B'$ and $T_{NI} = T'_{NI}$ were not enforced and the effective critical temperatures differed from T_{NI}^0 , the observed first-order temperature (at which C_p is a maximum).

Table IV shows the results of these N - I least-squares fits. The data in the nematic phase yield fits which are quite consistent with $\alpha' = \frac{1}{2}$ at both 1 atm and 500 bar. However, the values of χ^2_{ν} are high (relative to those at the N - $\text{Sm}A$ transition) due to systematic trends in the deviations over the entire range of t . The data in the isotropic phase yield fits characterized by extremely broad χ^2_{ν} minima, making a definitive determination of α impossible.⁴¹ If one carries out fits with $\alpha = \alpha'$ fixed at $\frac{1}{2}$, the resulting amplitude ratio A'/A is found to be 2.72 at 1 atm and 2.88 at 500 bar. These values are quite different from the ratio $A'/A \approx 8$ observed at the tricritical point in the ^3He - ^4He system.⁴² In view of the A'/A values and the fact that free fits in the isotropic phase give α values somewhat lower than $\frac{1}{2}$, quasitricritical behavior cannot be clearly established from these heat-capacity data.

ACKNOWLEDGMENTS

This work was supported by NSF Grant No. DMR 76-80895-A02, an NSF Fellowship to G.B.K., and a NATO Postdoctoral Fellowship to K.J.L.

- ¹W. L. McMillan, *Phys. Rev. A* **4**, 1238 (1971).
- ²P. G. de Gennes, *Solid State Commun.* **10**, 753 (1972); *Mol. Cryst. Liq. Cryst.* **21**, 49 (1973).
- ³B. I. Halperin, T. C. Lubensky, and S.-K. Ma, *Phys. Rev. Lett.* **32**, 292 (1974).
- ⁴T. C. Lubensky and J.-H. Chen, *Phys. Rev. B* **17**, 366 (1978).
- ⁵D. Djurek, J. Baturic-Rubic, and K. Franulovic, *Phys. Rev. Lett.* **33**, 1126 (1974).
- ⁶P. E. Cladis, *Phys. Rev. Lett.* **31**, 1200 (1973).
- ⁷D. Armitage and F. P. Price, *Mol. Cryst. Liq. Cryst.* **38**, 229 (1977).
- ⁸K. C. Chu and W. L. McMillan, *Phys. Rev. A* **11**, 1059 (1975); L. Cheung, R. B. Meyer, and H. Gruler, *Phys. Rev. Lett.* **31**, 349 (1973); M. Delaye, R. Ribotta, and G. Durand, *ibid.* **31**, 443 (1973).
- ⁹J. D. Litster, J. Als-Nielsen, R. J. Birgeneau, S. S. Dana, D. Davidov, F. Garcia-Golding, M. Kaplan, C. R. Safinya, and R. Schaetzing, *J. Phys. (Paris)* **40**, C3-339 (1979).
- ¹⁰S. Torza and P. E. Cladis, *Phys. Rev. Lett.* **32**, 1406 (1974).
- ¹¹M. Delaye, *J. Phys. (Paris)* **37**, C3-99 (1976); C. C. Huang, R. S. Pindak, and J. T. Ho, *Solid State Commun.* **25**, 1015 (1978); F. Schneider, *Z. Naturforsch. Teil A* **33**, 601 (1978); K.-C. Lim and J. T. Ho, *Phys. Rev. Lett.* **40**, 944 (1978).
- ¹²A. J. Leadbetter, J. C. Frost, J. P. Gaughan, C. W. Gray, and A. Mosley, *J. Phys. (Paris)* **40**, 375 (1979).
- ¹³P. E. Cladis, R. K. Bogardus, and D. Aadsen, *Phys. Rev. A* **18**, 2292 (1978).
- ¹⁴C. W. Garland, G. B. Kasting, and K. J. Lushington, *Phys. Rev. Lett.* **43**, 1420 (1979).
- ¹⁵D. L. Johnson, C. F. Hayes, R. J. deHoff, and C. A. Schantz, *Phys. Rev. B* **18**, 4902 (1978).
- ¹⁶P. Sullivan and G. Seidel, *Phys. Rev.* **173**, 679 (1968); P. Handler, D. E. Mapother, and M. Rayl, *Phys. Rev. Lett.* **19**, 356 (1967).
- ¹⁷J. D. Baloga and C. W. Garland, *Rev. Sci. Instrum.* **48**, 105 (1977).
- ¹⁸C. W. Garland and J. D. Baloga, *Phys. Rev. B* **16**, 331 (1977).
- ¹⁹For solutions to many similar problems see H. S. Carslaw and J. C. Jaeger, *Conduction of Heat in Solids*, 2nd ed. (Clarendon, Oxford, 1959).
- ²⁰K. J. Lushington, G. B. Kasting, and C. W. Garland (unpublished); K. J. Lushington and C. W. Garland, *J. Chem. Phys.* (in press).
- ²¹A more complete description is given in G. B. Kasting, Ph.D. thesis (MIT, 1979) (unpublished).
- ²²A. Michels, J. V. Sengers, and L. J. M. Van De Klundert, *Physica (Utrecht)* **29**, 149 (1963); A. Michels, Hub. Wýker, and Hk. Wýker, *ibid.* **15**, 627 (1949); A. Michels, R. J. Lunbeck, and G. J. Wolkers, *ibid.* **24**, 659 (1958); A. Michels, J. M. Levelt, and G. J. Wolkers, *ibid.* **24**, 769 (1958).
- ²³In cases where the cell has even a small pinhole leak, dissolved argon causes the cell to "blow up" upon depressurization.
- ²⁴G. B. Kasting, C. W. Garland, and K. J. Lushington, *J. Phys. (Paris)* (in press).
- ²⁵F. T. Lee, H. T. Tan, Y. M. Shih, and C. W. Woo, *Phys. Rev. Lett.* **31**, 1117 (1973).
- ²⁶P. G. de Gennes, *The Physics of Liquid Crystals* (Wiley, Oxford, 1974), p. 326.
- ²⁷D. Brisbin, R. deHoff, T. E. Lockhart, and D. L. Johnson, *Phys. Rev. Lett.* **43**, 1171 (1979).
- ²⁸D. Johnson (private communication).
- ²⁹Delaye (see Ref. 11) reported a value of 32 J mol⁻¹ for the DSC enthalpy of this transition. F. Hardouin, G. Sigaud, M.-F. Achard, and H. Gasparoux, *Ann. Phys. (Paris)* **3**, 381 (1978), reported a value of 26 J mol⁻¹. We also measured the enthalpy of this transition using a Perkin-Elmer DSC-2 and obtained a value of 60 J mol⁻¹. The difference between our result and the earlier values is most likely due to the choice of base line.
- ³⁰P. R. Bevington, *Data Reduction and Error Analysis for the Physical Sciences* (McGraw-Hill, New York, 1969).
- ³¹Since each data point has associated with it both an error in C_p and in T , a propagation-of-errors treatment leads to the expression $\sigma_i^2 \approx \sigma_{C_p}^2 + [\alpha A |t|^{-\alpha} / (T - T_{NA})]^2 \sigma_T^2$ for the variance of each point. However, σ_T is quite small for our experiment (<0.5 mK) and its effect is offset by the fact that σ_{C_p} tends to decrease near the transition as the temperature increments become smaller, possibly due to a more stable domain pattern in the sample. Hence, we have chosen to use equal weights for all fits except those with $|t|_{\min} = 1 \times 10^{-5}$, in which case the above expression was used with $\sigma_T = 0.2$ mK.
- ³²A quantitative estimate of the maximum error introduced into the C_p values by finite T_{ac} amplitudes is +0.6% for a 9 mK peak-to-peak oscillation centered at $|t| = 3 \times 10^{-5}$ and +1.2% for $|t| = 2 \times 10^{-5}$. See Ref. 21 for details.
- ³³A. Aharony and G. Ahlers, *Phys. Rev. Lett.* **44**, 782 (1980).
- ³⁴D. Davidov, C. R. Safinya, M. Kaplan, R. Schaetzing, R. J. Birgeneau, and J. D. Litster, *Phys. Rev. B* **19**, 1657 (1979); J. D. Litster, R. J. Birgeneau, M. Kaplan, C. R. Safinya, and J. Als-Nielsen, *Ordering in Strongly Fluctuating Condensed Matter Systems* (NATO Advanced Study Institute, 1979) (in press).
- ³⁵P. C. Hohenberg, A. Aharony, B. I. Halperin, and E. D. Siggia, *Phys. Rev. B* **13**, 2986 (1976), and references cited therein.
- ³⁶K. Mueller, G. Ahlers, and F. Pobell, *Phys. Rev. B* **14**, 2096 (1976); G. Ahlers (private communication).
- ³⁷P. G. de Gennes, *Mol. Cryst. Liq. Cryst.* **12**, 193 (1971); *Phys. Lett. A* **30**, 454 (1969).
- ³⁸P. H. Keyes, *Phys. Lett. A* **67**, 132 (1978).
- ³⁹C. Fan and M. J. Stephen, *Phys. Rev. Lett.* **25**, 500 (1970); R. G. Priest, *Phys. Lett. A* **47**, 475 (1974).
- ⁴⁰P. H. Keyes and J. R. Shane, *Phys. Rev. Lett.* **42**, 722 (1979).
- ⁴¹This statement applies as well to earlier work on MBBA: G. Koren, *Phys. Rev. A* **13**, 1177 (1976).
- ⁴²S. T. Islander and W. Zimmermann, Jr., *Phys. Rev. A* **7**, 188 (1973).